

Implications of direct detection experiments in search of mirror dark matter in Galaxy

Mohammad Tousif^a

^aDepartment of Physics & Astronomy, University of New Mexico, Albuquerque, 87131, NM, USA

E-mail: tousif@unm.edu

Abstract. We explore the possibilities of the mirror dark sector and its potential discovery in present and future experiments. Certainly, the mirror dark matters are isomorphic to the standard model lives in the hidden dark sector, and can be investigated in direct detection experiments if kinetic mixing interaction with ordinary matter exists. In this work, we study mirror electrons and mirror nuclei dark matter kinetic mixing interactions with the germanium and xenon targets. We estimate an upper limit on kinetic mixing $\epsilon \leq 10^{-9}$ at 95% C.L. for mirror electrons in dark plasma at local temperature ranges from 0.1 to 0.3 KeV. This limit manifests strong agreement with the experimental bound from LUX, and appreciably constrain the parameter space for the mirror electrons temperature below 0.3 KeV in the Milky Way halo around spiral galaxies. For mirror nuclei dark matter potentially viable parameter space on kinetic mixing of 10^{-11} to $4 \cdot 10^{-10}$ can be probed at 95% C.L for the mirror carbon, mirror oxygen to mirror neon compositions in halos within the mirror dark matter theory. In addition, we examine the dependence of the mirror nuclei dark matter scattering rate on the choice of halo model parameters, mirror nuclear form factors and demonstrate how these choices propagate to the predicted events and kinetic mixing sensitivity limits. We find the choice of halo model parameters affects the predicted sensitivity up to (15 – 71)% and parameterizations in nuclear form factor can lead to less than 2% effect on kinetic mixing sensitivity in the allowed parameter space over the mass scale (11 – 20) GeV. Analyzing all these aspects, we forecast direct detection experiments are highly sensitive and will allow a test of the mirror dark matter theory.

Keywords: mirror dark matter, direct detection

Contents

1	Introduction	1
2	Mirror dark matter in the galaxy	2
3	Halo model	3
4	Mirror dark matter scattering formalism	5
4.1	Mirror nuclei dark matter scattering rate	5
4.2	Mirror electrons dark matter scattering rate	8
5	Implications for direct detection	10
5.1	Germanium detector	11
5.2	Xenon detector	12
6	Results and discussion	12
6.1	Mirror electrons dark matter kinetic mixing limits	13
6.2	Mirror nuclei dark matter kinetic mixing limits	14
7	Conclusion	17
A	Mirror nuclear form factors and kinetic mixing sensitivity	17
B	Lindhard model	18

1 Introduction

The convincing observations of galactic rotation curves [1] in the twentieth century left significant clues about the existence of a new form of matter in the universe popularly known as dark matter (DM). DM is an exotic name with a simple meaning: it is non-radiant therefore dark and non-baryonic in the context of the standard model. The nature of dark matter (DM) is unknown to date and is considered one of the remaining questions to the physics community. In the past, tremendous efforts have been made to disclose the properties of DM and their cosmological origin. In recent times vast experimental effort has been going on [2–4] and several experiments are already under construction to join the direct detection class [5, 6] to discover the mysterious DM. Traditionally direct detection experiments operate deep underground to ensure the maximum background rejection. The invaluable channel for discovery is the nuclear and electronic recoil events induced by DM particles in the detector. Many of the mid and large-scale experiments are searching for weakly interacting massive particles (WIMPs), a theoretically well-motivated candidate that miraculously satisfies the PLANCK observations of dark matter density in the lambda cold dark matter formulation [7]. Interestingly a significant range of WIMP parameter space has already been excluded by many of the direct detection experiments [8]. As a result, interest in other theoretical models has increased from both theory and experimental points of view. Optimistically there are a plethora of hypotheses on dark matter [9, 10]. One such hypothesis is based on a mirror-dark sector with mirror symmetry. For the first time, the concept of mirror symmetry

was introduced in understanding the parity violation in weak interaction of the standard model[11]. It has been emphasized if mirror symmetry is respected by nature, then there is likely to exist a mirror world that would completely replicate the ordinary world. In this scenario, one would expect mirror electrons and mirror quarks to be the fundamental constituents of mirror matter, and mirror atoms are made of mirror nucleon (i.e. mirror proton, mirror neutron). Similar arguments for the existence of a mirror dark sector come from the study of neutron oscillations, more detail can be found in the reference [12]. The mirror dark sector is fascinating and mirror particles could be the potential candidates for DM which must be confirmed or ruled out by the direct detection experiment. In this work, it is supposed that mirror matter forms part of dark matter in the galaxy and we address physics related to the mirror electromagnetic and standard electromagnetic interaction with a possible kinetic mixing hence any features of mirror weak and strong along with standard weak and strong interactions are irrelevant in our analysis. We extensively study the impact of elastic mirror DM scattering on germanium and xenon targets for hypothetical process ($A' + A \rightarrow A' + A$) which warrants a firm investigation of mirror dark matter signals in direct detection experiments. Interestingly only a few attempts have been made in search of mirror dark matter in the context of direct detection as per the literature record.

We coordinated our work as follows. In section § 2 we begin with an overview of mirror dark matter in the galaxy. In § 3, we discuss the Halo model and associated astrophysical and cosmological parameters relevant to mirror DM. In section § 4, we thoroughly discuss the scattering formalism of mirror dark matter with standard model targets where we explore mirror nuclear form factors and other various ingredients that appear in the nuclear and electronic recoil rates estimation. In section § 5 we bridge theory predictions with experiments incorporating essential features of direct detection to draw a meaningful outcome of theory. We summarize our results in section § 6. Finally, we give a conclusion in section § 7.

2 Mirror dark matter in the galaxy

Certainly, the mirror dark matters are isomorphic to the standard model lives in the hidden dark sector, can participate in kinetic mixing interaction with the standard model (SM) ordinary matter. The total lagrangian density including the dark sector and kinetic mixing between SM and dark sector can be described as [13, 14],

$$\mathcal{L}_{\mathcal{T}} = \mathcal{L}_{SM}(e, \mu, d, \gamma, \dots) + \mathcal{L}_{\mathcal{D}}(e', \mu', d', \gamma', \dots) + \mathcal{L}_{\mathcal{M}} \quad (2.1)$$

$$\mathcal{L}_{\mathcal{M}} = -\frac{\epsilon}{2} F^{\mu\nu} F'_{\mu\nu} \quad (2.2)$$

where $\mathcal{L}_{\mathcal{M}}$ represents the massless standard photon and massless mirror photon kinetic mixing. Here $F^{\mu\nu} = \partial^\mu A^\nu - \partial^\nu A^\mu$ is the standard electromagnetism field tensor and $F'_{\mu\nu} = \partial^\mu A'^\nu - \partial^\nu A'^\mu$ is the mirror electromagnetism field tensor respectively. \mathcal{L}_{SM} has a gauge symmetry $SU(3)_C \otimes SU(2)_L \otimes U(1)_Y$ and the mirror dark sector represented by the lagrangian $\mathcal{L}_{\mathcal{D}}$ presumed to have mirror particles identical to standard model particles with $SU(3)'_C \otimes SU(2)'_L \otimes U(1)'_Y$ gauge symmetry. This tells us that mirror matter particles participate in mirror strong, weak and electromagnetic interactions and they never participate in standard model gauge interactions[15]. The kinetic mixing of $U(1)_Y$ in SM electromagnetism and $U(1)'_Y$ in mirror sector can induce mirror charge $\epsilon Z' e'$ to the mirror particles. In our work, we focus on kinetic mixing interaction of the dark sector with the standard sector contained within term $\mathcal{L}_{\mathcal{M}}$ with an application to the discovery of kinetic mixing interaction

in the direct detection experiments. We are motivated by the idea of mirror dark matter in the galaxy made of single elemental compositions i.e H', He', C', O', Ne', Mg', Si', Fe'. We highlight the possible benchmark values of mirror dark matter compositions in the solar neighborhood in Table 1.

Mirror Compositions	H' (%)	He' (%)	C' (%)	O' (%)	Fe' (%)
H', He'	25	75	-	-	-
H', He', C', O'	12.5	75	7	5.5	-
H', He', C', O', Fe'	20	74	0.9	5	0.1

Table 1. Mirror dark matter abundance in the solar neighborhood [16].

The chemical composition of mirror matter heavier than primordial nuclei H', He' can be present in the halos around spiral galaxies under several assumptions. One such assumption is motivated by the fact that heavy mirror nuclei (i.e Fe') are produced in stars and propel in the galaxy by supernova explosions thereby validate the idea of having heavy mirror atoms in the halos. Besides that halos contain moderately heavy C', O', and Ne' since they are produced in the CNO cycle in mirror stars. In addition, the idea of mirror electrons come from the plasma dark matter in the spiral galaxies like our Milky Way. It is believed that dark matter in spherically symmetric halos may take the form of a dark plasma consisting of mirror electrons and mirror nuclei i.e. H', He', O', Fe' etc [17, 18]. Mirror DM is dissipative in nature and assumed to have evolved in time. Of late it maintains a steady state configuration balancing heating and cooling rates. Considering mirror plasma in Milky Way is dominated by single element, the possible bounds on the kinetic mixing parameter ϵ with significant astrophysical uncertainties can be written as [17–20];

$$10^{-11} \leq \epsilon \sqrt{\xi_{A'}} \leq 4 \times 10^{-10} \quad (2.3)$$

Indeed, kinetic mixing [13] is necessarily required for the existence of small -scale structures and astrophysical considerations, therefore, providing a conservative limit on the kinetic mixing which is fairly given by the setting in eq.(2.3). We thoroughly examine this kinetic mixing bound using accessible nuclear and electron recoil events in current and forthcoming direct detection experiments. Here ϵ is one of the major parameters that can potentially affect the interaction rates in detectors. Besides that, mirror DM particles velocity distribution in halo and its associated parameters which enter the scattering rates explicitly needed to be accounted for. We give more detail on halo model in the following section.

3 Halo model

We consider a halo is composed of mirror DM particles in a thermal medium with an equilibrium temperature T and characteristic velocity dispersion v_0 is the direct measure of the thermal equilibrium in halos. In a canonically isothermal halo, we expect mirror DM particles to be trapped in the galactic field, and their velocity distributions can be treated as Maxwellian. With these assumptions, we can write the velocity distribution function for the mirror DM particles as follows [21],

$$f(\vec{v}, \vec{v}_E) = \begin{cases} \frac{1}{N} \left(e^{-(v+v_E)^2/v_0^2} \right) & v < v_c \\ 0 & v > v_c \end{cases} \quad (3.1)$$

where v is the velocity of mirror DM which is equivalent to v_{min} and v_c is the cutoff speed of mirror DM particles similar to galactic escape speed (v_{esc}) of WIMPs [22]. Here N is the normalization constant which can be found by setting the integral $\int f(v)d^3v = 1$. Here $v_E(t)$ represents the earth velocity with respect to the galactic rest frame and the time dependence carry the meaning of Earth's revolution around the sun. Including the effect of $v_E(t)$ mirror DM velocity distribution yields,

$$\zeta_{A'}(v_{min}(E_R), t) = \int_{v_{min}}^{\infty} f(\vec{v}, \vec{v}_E) \frac{d^3v}{v} \quad (3.2)$$

$v_E(t)$ is given by [23],

$$v_E(t) = v_s + bv_{\oplus} \cos[w(t - t_0)] \quad (3.3)$$

where v_s is the velocity of the sun in the galactic rest frame i.e. $v_s \approx 232$ km/s. We use the speed of the Earth's orbit to be $v_{\oplus} = 30$ km/s [24] and $\omega = \frac{2\pi}{T}$ with $T = 1$ year and $t_0 = 152$ (June 2nd) on which velocity of earth concerning mirror DM is maximally identical to WIMPs. Here t is the days in a year on which the experiments will be carried out. On simplifying the velocity integral in eq.(3.2), an analytical solution in the limit ($v_c \rightarrow \infty$) can be obtained as,

$$\zeta_{A'}(v_{min}(E_R), t) = \frac{N}{2\pi^{3/2}v_0(A')^3v_E} [erf(y_m + y_E) - erf(y_m - y_E)] \quad (3.4)$$

where we define $y_m = \frac{v_{min}}{v_0(A')}$ and $y_E = \frac{v_E}{v_0(A')}$ with normalization $N = \pi^{3/2}v_0(A')^3$. Here $v_0(A')$ is the velocity dispersion which can be determined from the hydrostatic equilibrium in halo with temperature $T = \frac{1}{2}\bar{m}v_{rot}^2$ given that the Milky Way galactic rotational velocity v_{rot} . In principles, v_{rot} may range $190 \leq v_{rot} \leq 250$ km/s [20]. For a mean mass of mirror DM particles in the completely ionized halo, one can estimate the velocity dispersion to be,

$$v_0(A') = \sqrt{\frac{2T}{M_{A'}}} = \sqrt{\frac{\bar{m}}{M_{A'}}}v_{rot} \quad (3.5)$$

In a homogeneous plasma consisting of H', He', e' , mean mass of mirror DM particles can be written as [25],

$$\bar{m} = \frac{\sum n_{A'}M_{A'}}{\sum n_{A'}} = \frac{n_{He'}M_{He'} + n_{H'}M_{H'} + n_{e'}M_{e'}}{n_{He'} + n_{H'} + n_{e'}} \quad (3.6)$$

Further, we assume the Milky Way mirror plasma to be charged neutral. With this assumption, the mirror electron number density $n_{e'}$ can be computed as,

$$n_{e'} = n_{H'} + 2n_{He'} \quad (3.7)$$

In the case of complete ionization, we find electron number density in mirror plasma to be,

$$n_{e'} = \frac{\rho}{M_u} \sum_{Z=H', He'} \frac{X_Z n_Z}{A_Z} = \frac{\rho}{M_u} \left(1 - \frac{Y_{He'}}{2}\right) \quad (3.8)$$

provided $X_H + Y_{He'} \equiv 1$ in a hydrogen and helium-dominated mirror plasma with n_Z as the number of free electrons in Z type of atoms and X_Z is the corresponding mass fractions in a mirror plasma. Here M_u represents the mass of 1 amu which is equivalent to the mass of hydrogen. Since the mass of mirror hydrogen and mirror helium are much higher than the

mirror electrons mass i.e $M_H, M_{He'} \gg M_{e'}$ and $M_{He'} = 4M_{H'}$, with these considerations, the charge neutrality reads,

$$\bar{m} \approx \frac{M'_H}{2 - \frac{5}{4}Y_{He'}} \quad (3.9)$$

given that $Y_{He'}$ is the mirror helium fraction [25],

$$Y_{He'} = \frac{n_{He'}M_{He'}}{n_{He'}M_{He'} + n_{H'}M_{H'}} \quad (3.10)$$

Assuming the kinetic mixing $\epsilon = 10^{-10}$ and mirror helium fraction $Y'_{He} \equiv 1$, we find the mean mass of mirror DM particles to be $\bar{m} \approx 1.25$ GeV in a Milky Way halo. Therefore, we fix the mean mass of DM particles to 1.25 GeV in our halo model. In this layout, the lightest mirror DM particles have higher velocities than the heaviest ones. Notice mass-dependent velocity dispersion has smaller values in halos than the distribution expected for collisionless cold dark matter (CDM). Usually collisionless CDM particles possess much higher velocity dispersion and often approach the galactic rotational velocity i.e. $v_0 \equiv v_{rot}$. Another crucial parameter in the halo model is the earth velocity $v_E(t)$. It can be estimated for different days in a year with the approximated value of $v_E \approx v_s \pm 15$ km/s. The time dependence in the earth velocity would cause systematic variations in the recoil events over the background in direct detection experiments [26–28].

In the case of the mirror electrons from galactic plasma, we extrapolate our assumption that mirror electrons can maintain a local temperature up to 1 KeV in a mirror plasma and, therefore attain the highest velocity dispersion than mirror nuclei. We overlook the effect of earth velocity $v_E(t)$ for mirror electrons velocity distribution in the detector frame takes the form,

$$\zeta_{e'}(v_{min}(E_R), t) = \int_{v_{min}}^{\infty} f_{e'}(v) \frac{d^3v}{v} \quad (3.11)$$

provided mirror electron velocity dispersion $v_0(e') = \sqrt{\frac{2T}{m_{e'}}}$ with $N = \pi^{3/2}v_0(e')^3$ and v_{min} is the minimum of mirror electrons velocity which can be obtained from nonrelativistic scattering process that we show later this section. As we can see both mirror DM and mirror electrons velocity distributions depend on the astrophysical parameters and their associated uncertainties which can importantly affect the model predictions of signal events. Besides interaction rates of mirror DM particles with the target nucleus have direct consequences to spin-independent helm form factors $F^2(q)$, which contains the nuclear physics properties i.e. effective nuclear radius and nuclear skin thickness of mirror DM nuclei as well as SM target nuclei. In the following section, we give details on mirror DM scattering formalism and briefly discuss all these aspects in quantifying the recoil rates.

4 Mirror dark matter scattering formalism

In this segment, we briefly review the theory of mirror dark matter scattering with standard model targets. In particular, we discuss mirror nuclei DM and mirror electron scattering assuming the scattering occurs within non-relativistic regimes in the lab frame.

4.1 Mirror nuclei dark matter scattering rate

If an incoming mirror nuclei with a minimum velocity v_{min} scatters off an ordinary nuclei assumed initially at rest, then the ordinary nucleus would have the momentum transfer

$q \leq 2\mu_T v_{min}$ yielding a recoil E_R . We ensure complete coherence across the kinetically accessible region of momentum transfer by imposing the condition,

$$\mu_T \ll \frac{1}{2v_{min}R} \quad (4.1)$$

where $\mu_T = \frac{M_{A'}M_T}{M_{A'}+M_T}$ is the reduced mass of the two body system i.e. mirror nuclei N' and target N_T . Here R is the measure of effective nuclear radius of the target with mass M_T . For a mirror DM having mass $M_{A'}$, a minimum incoming speed in lab frame can found using the non-relativistic kinematics,

$$v_{min} = \sqrt{\frac{(M_T + M_{A'})^2 E_R}{2M_T M_{A'}^2}} \quad (4.2)$$

We are interested in the low energy elastic scattering process relevant to direct detection in the detector rest frame,

$$N' + N_T \rightarrow N' + N_T \quad (4.3)$$

Essentially, the above scattering is a Rutherford type in which an electrically charged mirror nucleus with the mirror charge Z' encounters ordinary nucleus with charge Z irrespective of the internal structure of the participant particles in the scattering. Ensuring complete coherence, the differential scattering cross section in the low energy regime can be estimated as following [29, 30]:

$$\frac{d\sigma_{A'}}{dE_R} = \frac{2\pi\epsilon^2\alpha^2 Z^2 Z'^2 F_A^2 F_{A'}^2}{M_T E_R^2 v_{min}^2} \quad (4.4)$$

where α represents the fine structure constant and $F_{A'}(F_A)$ are form factors of the mirror (ordinary) nuclei. The scattering between target nuclei and mirror dark matter cannot be treated as point-like as both target nuclei and mirror nuclei dark matter have nuclear charge distributions due to their finite size of the nucleus. It is mandatory to introduce a charge density model that can account for salient features of the nucleus and can provide acceptable nuclear form factors describing essential nuclear properties. In the scattering process assumed in eq.(4.3), the form factors for both mirror and ordinary nuclei can be approximated to the spin-independent helm form which is obtained from the Fourier transform of Wood-Saxon nuclear charge density distribution with nuclear radius R and nuclear skin thickness s can be written as the function of three momentum transfer q in the scattering [31, 32],

$$F(q^2) = \frac{3j_1(qR)}{qR} e^{-\frac{(qs)^2}{2}} \quad (4.5)$$

where j_1 is the spherical Bessel function of the first kind given by,

$$j_1(qR) = \frac{\sin(qR) - qR \cos(qR)}{(qR)^2} \quad (4.6)$$

A choice of R and s can be made as discussed by Engel [33, 34],

$$R = \sqrt{\tilde{R}^2 - 5s^2} \quad (4.7)$$

with $\tilde{R} = 1.2A^{1/3}$ fm and $s = 1$ fm. Another choice on R and s can be implemented using Lewin-Smith parametrization [35],

$$R = \sqrt{c^2 + \frac{7}{3}\pi^2 a^2 - 5s^2} \quad (4.8)$$

$s = 0.9$ fm, $a = 0.52$ fm and $c = (1.23A^{1/3} - 0.6)$ fm. The measure of an effective nuclear radius and skin thickness of a mirror(ordinary) nuclei are the crucial entities in the computation of the helm factors as they directly scales with the differential scattering cross-section. It is evident that the choice of R and s parameters can have a notable effect on nuclear recoil rates due to the different parameterizations. We would like to suggest that nuclei relevant for direct detection, there exist some differences between these form factors that we display in Fig.(1). Lewin-Smith helm factor parameterization is widely used in the direct detection experiments. Additionally, we study parameterization by Engel and we make a meaningful comparison of kinetic mixing sensitivity on these choices of parameterizations which we show in our results.

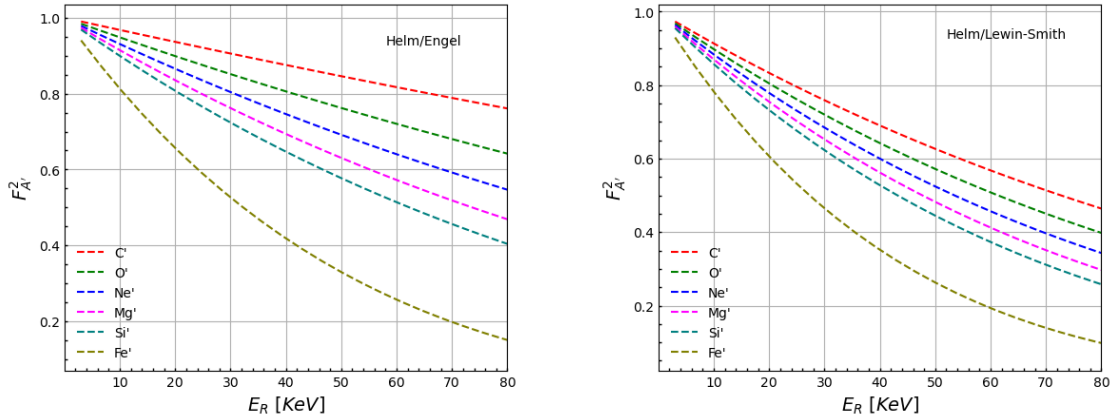


Figure 1. Mirror nuclei form factors on xenon target for spin-independent Helm parameterizations. Helm/Engel computed from eq.(4.7) and Helm/Lewin-Smith computed from eq.(4.8).

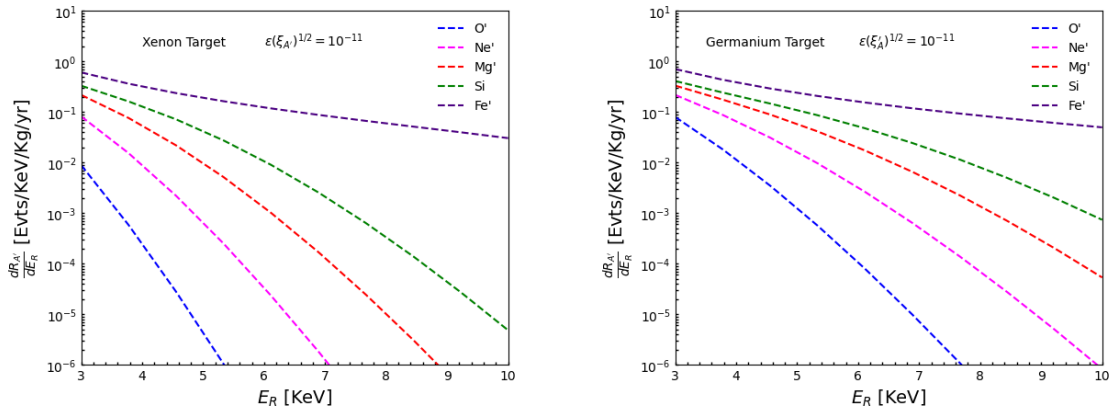


Figure 2. Mirror dark matter recoil rate at xenon detector ($E_{th} = 3$ KeV) and germanium detector $E_{th} = 1$ KeV with kinetic mixing $\epsilon = 10^{-11}$ computed using Lewin-Smith parameterization.

The recoil rate of Mirror DM particle off a SM target nuclei is given by,

$$\frac{dR_{A'}}{dE_R} = N_T n_{A'} \int_{v_{min}} \frac{d\sigma_{A'}}{dE_R} f(v, v_E) v d^3v \quad (4.9)$$

$$\frac{dR_{A'}}{dE_R} = N_T n_{A'} \left(\frac{2\pi\epsilon^2\alpha^2 Z^2 Z'^2 F_A^2 F_{A'}^2}{M_T E_R^2} \right) \zeta_{A'}(v_{min}(E_R), t) \quad (4.10)$$

We are interested in estimating mirror signal events that are caused by the maximum and minimum variations of earth velocity in the detector rest frame. Therefore, we pay attention to the time dependent recoil rate in eq.(4.10) that can potentially affect the expected mirror events as well kinetic mixing sensitivity however the daily modulation effect is not studied in this work. We denote the mirror dark matter density as $n_{A'} = \frac{\rho_{A'}}{M_{A'}}$, a typical value of $\rho_{A'} = 0.4 \text{ GeV/cm}^3$ [36] is used in numerical computation throughout this work.

4.2 Mirror electrons dark matter scattering rate

Like mirror nuclei DM, we consider mirror electrons scattering. Mirror electrons are sufficiently energetic to escape the mirror plasma in the galaxy and they are electrically charged in the presence of kinetic mixing can scatter off loosely bound electrons in the detector's target via two-body elastic scattering,

$$e' + e \rightarrow e' + e \quad (4.11)$$

Because of three momentum transfer among the mirror electron and loosely bound electrons in the scattering process, a KeV scale recoil is anticipated which can be measured in direct detection experiments. Essentially the mirror electron scattering process can only be valid for the loosely bound atomic electrons, i.e. those with binding energy E_B much less than recoil energy E_R . Naturally, it is a Coulomb scattering between two charged particles which is assumed to be spin-independent similar to scattering of mirror nuclei discussed in the preceding section. Approximating the loosely bound electrons in the target as free at rest relative to the incoming dark electrons having speed v_{min} , the cross section can be estimated as [29, 30],

$$\frac{d\sigma_{e'}}{dE_R} = \frac{2\pi\epsilon^2\alpha^2}{m_e E_R^2 v_{min}^2} \quad (4.12)$$

$$v_{min} = \sqrt{\frac{(m_e + m_{e'})^2 E_R}{2m_e m_{e'}^2}} \quad (4.13)$$

Mirror electrons mass and ordinary electrons mass are assumed to be equal i.e $m_e = m_{e'}$ this leads to $v_{min} = \sqrt{\frac{2E_R}{m_e}}$. Here E_R is the measure of recoil in the scattering in eq.(4.11). The differential scattering rate is given by,

$$\frac{dR_{e'}}{dE_R} = N_T N_f n_{e'} \int_{v_{min}} \frac{d\sigma_{e'}}{dE_R} f_{e'}(v) v d^3v \quad (4.14)$$

Considering $Y_{He'} = 1$ for kinetic mixing $\epsilon = 10^{-10}$, we estimate mirror electron number density in mirror plasma to be $n_{e'} \approx 0.21 \text{ cm}^{-3}$ in the lab frame. Here N_T represents the number of target nuclei per kilogram. Introducing the differential scattering cross-section of mirror electron off ordinary electron and setting,

$$\frac{2\pi\epsilon^2\alpha^2}{E_R^2 v_{min}^2} = \lambda \quad (4.15)$$

we write the general form of the differential interaction rate as follows,

$$\frac{dR_{e'}}{dE_R} = N_T N_f n_{e'} \frac{\lambda}{E_R^2} \zeta_{e'}(v_{min}(E_R), t) \quad (4.16)$$

In determining the mirror recoil rate N_f is one of the key parameters required to be precisely accounted for. In our notation, N_f represents the loosely bound electrons available in the detector target i.e. Ge, Xe, etc. N_f solely depends on the electronic configuration of materials, we consider electrons to be loosely bound in a material for which the binding energies (E_B) are much smaller than electrons recoil in the detector i.e. $E_B \ll E_R$. In germanium, one could imagine 22 loosely bound electrons (18 from the K shell and 4 from the N shell). The binding energy of innermost M shell electrons is $E_B \approx 180$ eV (we use the electron binding energy information from the Lawrence Berkeley database) which is far below the threshold of (1-2) KeV in germanium detectors means they can be treated as free to be participated in scattering with mirror electrons. Using the same logic, one would expect a significantly higher number of loosely bound electrons in xenon as allowed by its electronic configuration. In xenon, the innermost M shell electron has $E_B = 1.1487$ which is quite below the threshold of (3-5) KeV of the modern-day xenon detector. As a result, 44 loosely bound electrons are accessible in the xenon target.

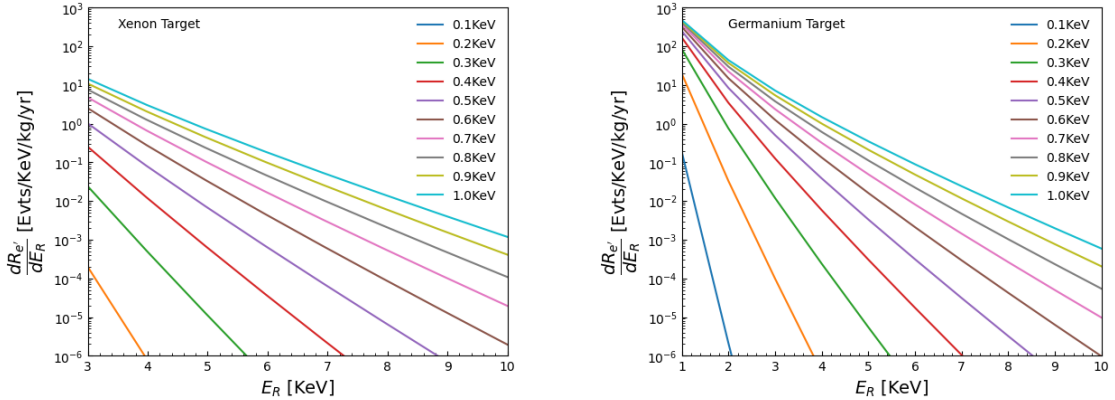


Figure 3. Mirror electron rate in xenon detector ($E_{th} = 3$ KeV) and germanium detector ($E_{th} = 1$ KeV) with the strength of kinetic mixing $\epsilon = 10^{-10}$ computed using eq.(4.16).

It can be seen for both mirror nuclei and mirror electrons, the recoil rates are inversely proportional to that of squared recoil energy which is completely different than WIMPs scattering rate [37, 38]. The satisfying reason for such a difference in the recoil rate can understood as follows: mirror DM particles interact electromagnetically permitting a photon-mirror photon kinetic mixing with a strength parameter ϵ and enough nuclear recoil is anticipated in a partially coherent scattering such that the signal is not excessively suppressed. This makes mirror dark matter a plausible candidate which can potentially give measurable recoil in direct detection experiments. So far, we have accomplished a theoretical description of interaction rates of mirror nuclei dark matter and mirror electrons. In the next section, we give implications of modern-day experiments in detecting mirror dark matter signals incorporating various experimental features.

5 Implications for direct detection

Goodman and Witten in their famous paper [39] first talked about the dark matter direct detection [39]. In direct detection experiments, the key idea is to study the scattering of mirror DM particles with target materials in the Earth based detector and extract information about their masses and couplings to the ordinary matter. It is expected that the induced electric charge of mirror DM particles can elastically scatter off ordinary nuclei yielding a nuclear or electronic recoil as per the kinematics discussed in § 4.1 and the majority of experiments are sensitive to record these recoils. For that we require big detectors with possibly a lower threshold similar to WIMPs search [40]. The reason for the low threshold is because mirror DM has a smaller differential scattering cross-section. For mirror compositions O' and Fe' , we estimate their differential scattering cross sections range $(5.03 \cdot 10^{-38} - 3.56 \cdot 10^{-45}) \text{ cm}^2/\text{KeV}$ and $(3.13 \cdot 10^{-36} - 8.85 \cdot 10^{-44}) \text{ cm}^2/\text{KeV}$ respectively in $(1 - 100) \text{ KeV}$ nuclear recoil in germanium target for an kinetic mixing $\epsilon = 10^{-11}$. Along with the detector characteristics the main strategy of direct detection is to smear model prediction with detector resolution which is customarily taken to be Gaussian in nature. We include the resolution effects as we are interested in making a meaningful outcome of theory in regard to experiments. The convoluted rate is given by,

$$\frac{dR_c}{dE_R}(E_R) = \int \mathcal{R}(E_R|E'_R) \frac{dR}{dE_R}(E'_R) dE'_R \quad (5.1)$$

where $\mathcal{R}(E_R|E'_R)$ is the resolution function with energy dependent detector resolution σ ,

$$\mathcal{R}(E_R|E'_R) = \frac{1}{\sqrt{2\pi}\sigma(E'_R)} e^{-\frac{(E_R - E'_R)^2}{2\sigma^2(E'_R)}} \quad (5.2)$$

With the signal model, the detector resolution is accounted for the deposited recoil by smearing theoretical distribution. We implement bin to bin folding method reconstructing the theoretical recoil rates in each bin, and the individual bin contributions are added up to get the total convoluted rates in the energy region of interest. Moreover, in these binned reconstructions detector efficiency must be considered to obtain actual convoluted rates. In the direct detection experiments, the detector's efficiency depends on the recoil energy. Including all these important effects, Ultimately recoil spectrum in an experiment can be written as follows,

$$\frac{dR_m}{dE_R}(E_R) = \kappa(E) \frac{dR_c}{dE_R}(E_R) \quad (5.3)$$

For the projected sensitivity estimation one can simply model the detector's efficiency in the following fashion,

$$\kappa(E_R) = \frac{\alpha}{\beta + \gamma e^{-E_R}} \quad (5.4)$$

where α, β, γ are the constant parameters that can be achieved from the fitting efficiency curves for various experimental detectors. For each of the detectors, we find the optimum value of the parameters α, β, γ that can sufficiently describe the efficiency curves over the recoil energy region of interest.

Ultimately the number of mirror dark matter events is an important ingredient in drawing the sensitivity of any detectors. For that, we calculate the total number of signal events

in a given energy interval $E_R \in (E_R^{min} - E_R^{max})$ as follows,

$$N_{Tot} = \int_{E_R^{min}}^{E_R^{max}} \chi_{eff} \cdot \frac{dR_m}{dE_R}(E_R) dE_R \quad (5.5)$$

here χ_{eff} is the effective exposure. The effective exposure is obtained by incorporating the exposure run with detection efficiency and selection cut efficiency. We present a brief study on state-of-the-art germanium and xenon detectors to obtain the necessary information about the detector characteristics in Table 2 and Table 3.

5.1 Germanium detector

Germanium detectors have been widely used in dark matter direct detection [41–43] and neutrino-less double beta decay experiments [44, 45]. MAJORANA is currently taking data. Due to the excellent detection efficiency and energy resolution strong background discrimination made MAJORANA an excellent detector for searching new physics at the KeV scale. A recent analysis on dark matter in low threshold region has been reported by the collaboration [46]. Since mirror electrons are sensitive to give nuclear recoil in KeV scale, we perform a similar analysis following the resolution technology of MAJORANA,

$$\sigma_M(E) = (a^2 + b^2 E + c^2 E^2)^{1/2} \quad (5.6)$$

where $a = 0.138$, $b = 0.017$ and $c = 0.00028$ are the fit parameters can be obtained from the paper [46]. For detection efficiency, we use a similar to MAJORANA.

Table 2. Essential experimental features of beta decay experiments with Germanium target

Experiment	MAJORANA	LEGEND
Active mass	37.5 kg	910 kg
Threshold (NR)	1 KeV	(1.3 - 4.7) KeV
Background (Events/Kg/KeV _{ee} /day)	$\approx 2.08 \times 10^{-1}$ [46]	-
Efficiency	eq.(5.4)	eq.(5.4)
Resolution	eq.(5.6)	eq.(5.6)

LEGEND is a forthcoming experiment¹, with a 1-ton germanium target that will provide 910 kg active experimental volume in search of neutrino-less double beta decay. The experiment is expected to run for 10 years, and is committed to achieving the best resolution and low backgrounds i.e ($\leq 10^{-5}$ [Counts/KeV/kg/year]) in the double beta decay region of interest in ^{76}Ge isotope, however, in the low energy region LEGEND might have more backgrounds, in future this statistics will be published by the collaboration. Albeit MAJORANA and LEGEND are designed for neutrino less double beta decay search, we strongly suggest these detectors are sensitive to mirror dark matter signals and could potentially look for nuclear and electronic recoil in the low energy region of the recoil spectrum. We present our analysis to 1 – 100 KeV region of interest sliced off 1 KeV bin width.

¹<https://legend-exp.org/science/legend-pathway/legend-1000>

5.2 Xenon detector

Ton-scale xenon detectors [47–49] have been proposed in the context of searching rare events i.e. dark matter and neutrino less double beta decay [50, 51]. The existing ton scale xenon detectors i.e LZ, PANDAX-4T, XENONnT with a low energy threshold and strong background discrimination, we find these detectors are highly sensitive for mirror nuclei dark matter kinetic mixing interaction which we show in the next section.

Table 3. Essential experimental features of direct-detection experiments with Xenon target

Experiment	XENONnT	LZ	PANDAX-4T
Active mass	5.9 ton	5.5 ton	3.7 ton
Threshold (NR)	3.3 KeV	3 KeV	5 KeV
Background (Events/Kg/KeV _{ee} /Year)	$\approx 1.14 \times 10^{-5}$ [52]	$\approx 2.35 \times 10^{-2}$ [53]	$\approx 10.21 \times 10^{-5}$ [54]
Efficiency	eq.(5.4)	eq.(5.4)	eq.(5.4)
Resolution	eq.(5.7)	eq.(5.7)	eq.(5.7)

In each of these three detectors listed above in Table 3, we choose the resolution like XENON1T as reported in the reference [55],

$$\sigma(E_{er}) = a' \cdot \sqrt{\frac{E_{er}}{KeV}} + b' \cdot \frac{E_{er}}{KeV} \quad (5.7)$$

with $a' = 0.31\sqrt{KeV}$ and $b' = 0.0037$ neglecting the small uncertainties in a', b' . We convert the electronic equivalent energy to nuclear recoil using Lindhard’s model detail can be found in the appendix § B and scan the 3 – 60 KeV energy region of nuclear recoil with a 1 KeV bin width. We accomplish background-free analysis assuming the maximum rejection of backgrounds in experiments however inclusion of background in real experimental data analysis would be paramount and it is beyond the scope of this theoretical work.

6 Results and discussion

In this section, we present the results from the mirror electron and mirror dark matter model that has been discussed throughout the main text. We obtain detailed statistics on signal events for the mirror dark matter and mirror electrons respectively with the choice of astrophysical and cosmological parameters in the halo model considering complementary among baseline design of various detectors and discuss the ability to probe the allowed parameter space at each and individual experiments. We forecast the sensitivity of the mirror dark matter kinetic mixing at the 95% confidence level in the selected energy region of interest.

6.1 Mirror electrons dark matter kinetic mixing limits

Our mirror electron model has three main parameters that can fully describe the physics: ϵ , m_e , and α and an auxiliary parameter T which is the measure of local mirror electron temperature in halos. We obtain a 95% confidence limit on the kinetic mixing parameter ϵ in the range $0.1 - 1$ KeV of local mirror electron temperature. The previous experimental constraint on ϵ comes from orthopositronium decays to invisible states in a vacuum where 90% upper limit on kinetic mixing placed as $\epsilon \leq 3.1 \times 10^{-7}$ [56]. For LEGEND and MAJORANA detectors, we notice that kinetic mixing above mirror electrons local temperature 0.3 KeV is excluded and more interestingly both these detectors recover the bounds set by LUX below a kinetic mixing of $\epsilon \leq 10^{-9}$ and consistent with previous observations [57].

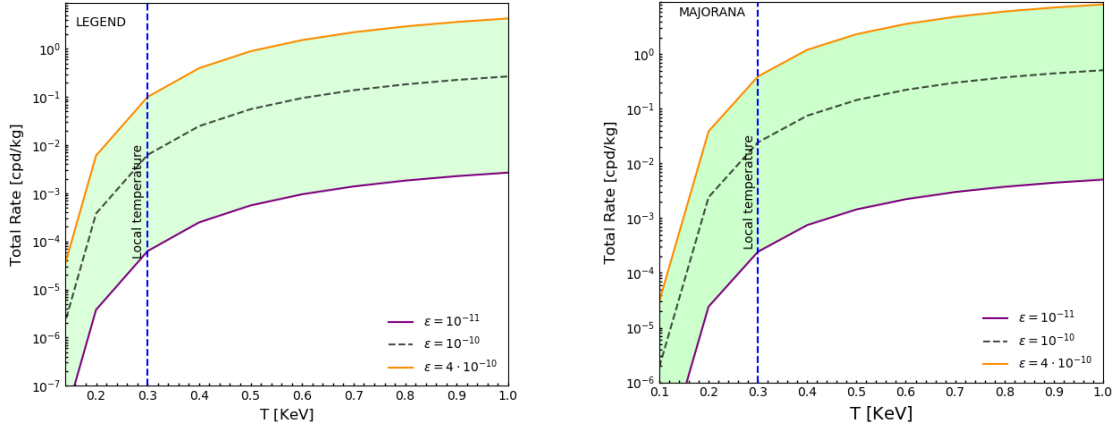


Figure 4. Total rate of mirror electron at germanium detector. Bands in lime color shows the allowed parameter space in eq.(2.3) within the mirror dark matter theory.

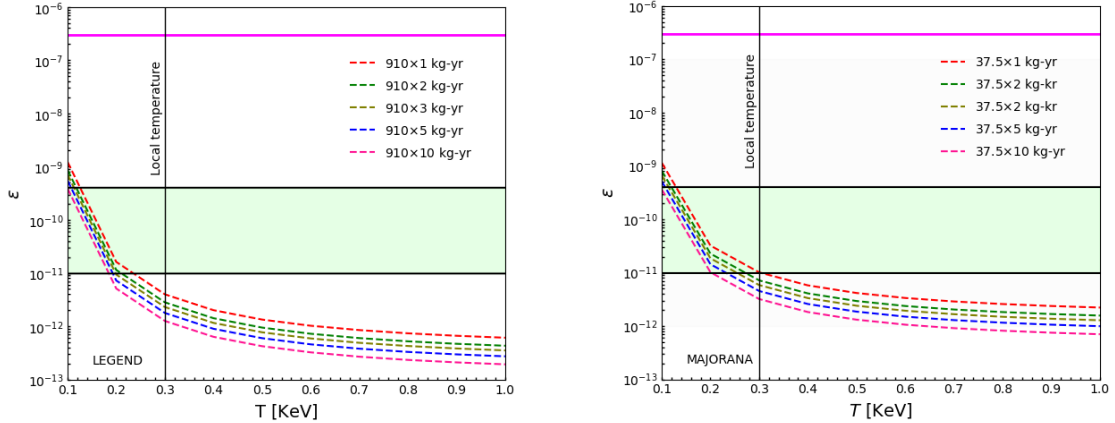


Figure 5. 95% exclusion plots at germanium detector with various exposures for mirror electrons dark matter. The horizontal shaded region in lime color shows the allowed parameter space in eq.(2.3) within the mirror dark matter theory. Magenta line (solid thick) is the upper bound from orthopositronium decay [56].

In germanium detectors, we expect a range of $(0.1 - 0.3)$ KeV local temperatures, theoretical limits on kinetic mixing interaction of $10^{-11} \leq \epsilon \leq 4 \cdot 10^{-10}$ can be probed

however this limit can be improved in bigger-sized germanium detector like LEGEND if the experiment attain a low threshold i.e. $E_{th} \approx 1.3$ KeV is close enough to MAJORANA with a less background in low threshold region. We notice in Fig.(5) that a germanium detector with a long exposure run can significantly constrain the parameter space below mirror electrons local temperature of 0.3 KeV. The mirror electrons model we presented here is complementary and seemingly worthwhile for the mid-scale experiment i.e. MAJORANA and future ton scale germanium detector i.e. LEGEND. At the next generation experiments with better resolution and better background discrimination with longer exposures i.e the kinetic mixing limits can be estimated with better precision and local temperature of the mirror electrons in halos around spiral galaxies will be constrained below 0.26 KeV. Our analysis indicates the kinetic mixing interactions can independently be discovered in germanium detectors and potentially mirror electrons recoil rates can be measured. We show model predictions of the mirror electron recoil rates in Fig.(4) in the allowed parameter space within the mirror dark matter theory.

6.2 Mirror nuclei dark matter kinetic mixing limits

We present sensitivity projection for hydrogen, and helium up to iron based on the model of mirror nuclei dark matter discussed in this work. It is interesting to note that all state-of-art xenon detectors are highly sensitive to record mirror signal events for moderately heavy mirror compositions C', O', Ne' as there is less kinematic suppression due to their larger masses but it will substantially exclude the significantly heavy mirror compositions i.e Mg', Si', Fe' despite of their least kinematic suppression. This means that heavier components than hydrogen and helium can potentially produce a larger signal in the xenon detector even if they are subdominant in abundance as listed in Table 1.

It can be seen Fig.(6) that LZ, XENONnT, PANDAX-4T, and LEGEND experiments in the mass region of 15 to 20 GeV exhibit a slightly better reach to the kinetic mixing sensitivity as all these detectors receive a significant number of events in selected energy bins however at higher energies, the tail of the mirror velocity distribution is strongly suppressed therefore less nuclear recoil is anticipated dropping sensitivity regardless of detector threshold, energy resolution and efficiency. Comparing between the $v_{rot} \in (190, 250)$ km/s, we see that our model results in the greatest events in all the ton size detectors for values $v_{rot} = 190$ km/s while it results in the smallest events for $v_{rot} = 250$ km/s, in both cases average value of earth velocity $v_E \equiv 235$ km/s is used. However, this scenario is different for variation in earth velocity concerning the galactic rest frame. Maximum earth's velocity yields lesser events for $v_{rot} = 250$ km/s and higher events for $v_{rot} = 190$ in comparison to mean galactic rotational velocity $v_{rot} = 220$ km/s. For the minimum earth's velocity, the trend is exactly the opposite. These behaviors are justified by the fact that velocity distribution is overall sensitive to changes across its associated halo model parameters which cause up to $(15 - 71)\%$ ² effect in kinetic mixing sensitivity either increment or decrement in the allowed region of parameter space over the mass scale of $(11 - 20)$ GeV that can be seen from the violet and yellow bands in Fig(7). It is clear that kinetic mixing sensitivity decreases as the maximum value of earth velocity i.e. $v_E = 246$ km/s is reached in June and kinetic mixing sensitivity increases as the minimum earth's velocity i.e. $v_E = 217$ km/s is achieved in December. This is because maximum earth velocity causes a significant rise in recoil rates that contribute

²Percentage change in kinetic mixing sensitivity is calculated in respect of $(v_E, v_{rot}) = (235, 220)$ km/s with the choices of sets $(v_E, v_{rot}) = (217, 220)$ km/s and $(v_E, v_{rot}) = (246, 220)$ km/s as shown in Fig(5) and Fig(6).

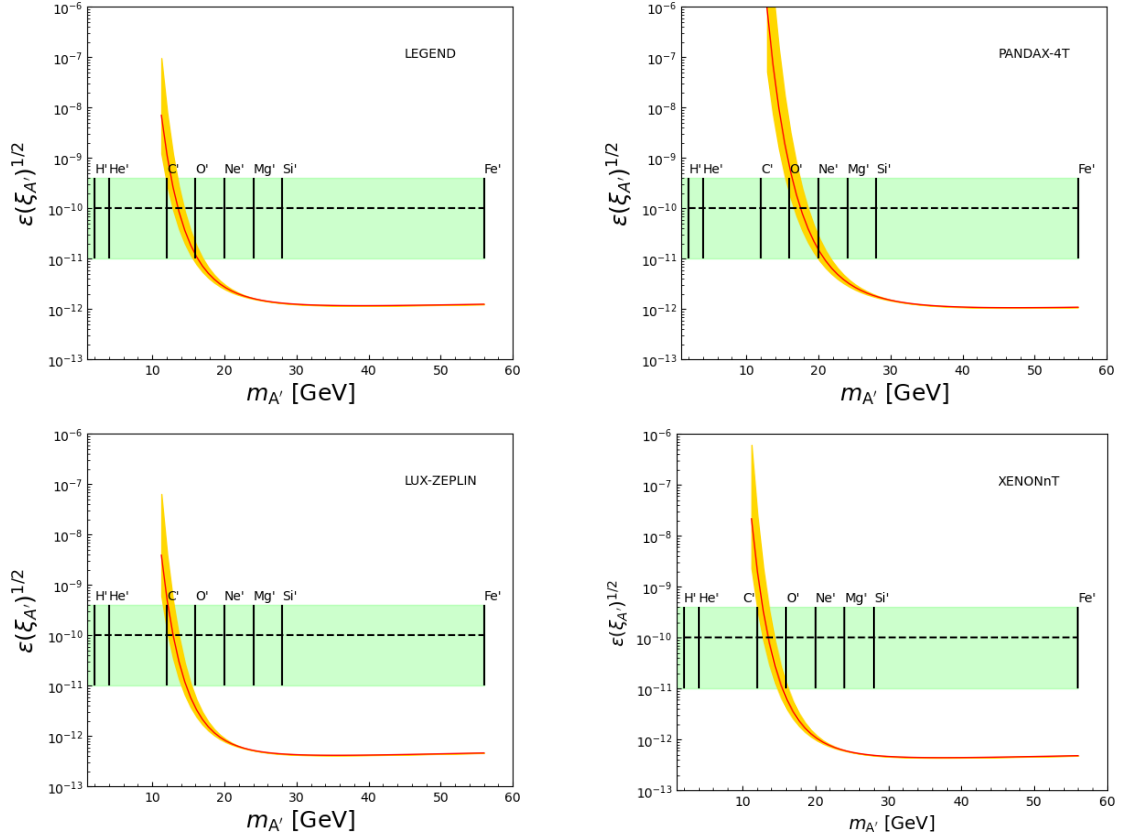


Figure 6. 95% exclusion plots for mirror dark matter kinetic mixing in ton-size experiments for one year of exposure. The horizontal shaded region in lime shows the existing mirror kinetic mixing bounds in eq.(2.3) within the mirror dark matter theory, yellow band corresponds $v_{rot} = (190 - 250)$ km/s. Red(solid) represents 220 km/s and lower and upper edge represents 250 and 190 km/s respectively in the interval of v_{rot} with average $v_E = 235$ km/s.

to enhancing the signal events and thereby decrease the kinetic mixing sensitivity as the predicted sensitivity limit inversely scales with the signal events and converse is true for minimum earth velocity. Thus, it is meaningful to observe the yellow band on top of the violet band in Fig.(7). This states that the choice of halo model parameters in the violet band will produce a lower limit on kinetic mixing than the yellow band across all the detectors. In each of these bands, solid lines show the mean value of the galactic rotational velocity of 220 km/s, and the edges of the individual band represent the range of $v_{rot} = (190 - 250)$ km/s. It is interesting to note that for both violet and yellow bands, edges are sufficiently close to mean solid lines, which means spreading out of earth velocity cannot cause the enormous change in kinetic mixing sensitivity in each band. We find the ton-size xenon detector can potentially probe the allowed parameter space irrespective of the choice of halo model parameters, C' , O' , Ne' compositions remain viable in the mass range of (11 – 20) GeV. We expect the forthcoming experiment LEGEND will be sensitive to mirror dark matter i.e. C' , O' and will provide complementary tests over existing state-of-art xenon detectors in the mass range (11 – 16) GeV. We also examine the choice of mirror form factors. The measure of nuclear radius and nuclear skin thickness associated with mirror dark matter, we observed these choices can cause up to (2 – 4)% increment in signal events. A 95% exclusion limits

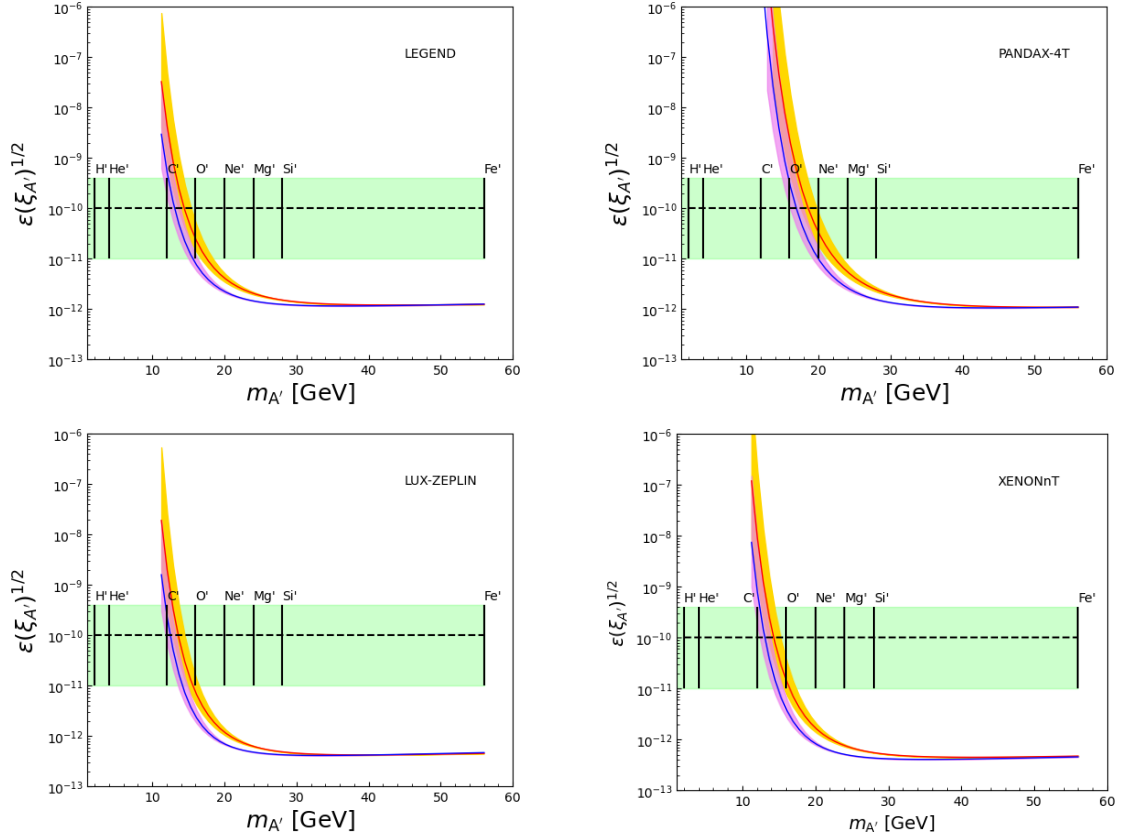


Figure 7. 95% exclusion plots for mirror dark matter kinetic mixing in ton-size experiments for a year of exposure. The horizontal shaded region in line shows the existing mirror kinetic mixing bounds in eqn.(2.3) within the mirror dark matter theory. Yellow band corresponds $v_{rot} = (190 - 250)$ km/s with $v_E = 217$ km/s (min). Violet band corresponds $v_{rot} = (190 - 250)$ km/s with $v_E = 246$ km/s (max). Red(solid) and blue(solid) line represents $v_{rot} = 220$ km/s. Lower and upper edge of the bands equivalent to v_{rot} interval respectively.

on the kinetic mixing sensitivity calculated using Lewin-Smith form factors generated within the Helm parameterization match the Engel form factors parameterization and the ratio of these estimated sensitivities is close to one in all the ton size detectors. Highlighting the 11-20 GeV region in the grey band as most of the detectors are sensitive in that region, we quantify sensitivity differs only by less than 2% as shown in Fig.(8). An example of 95% exclusion limit on ϵ for XENONnT is presented in Table 4 in appendix § A. Therefore, we suggest that either of the choices of parameterizations in mirror nuclear form factors will suffice in determining the kinetic mixing sensitivity and this limit is quite robust based on model predictions. Finally, we emphasize once the longer exposure data from current and forthcoming direct detection experiments start streaming, this type of analysis will be in an important place to ask how well the mirror kinetic mixing can be determined and how well direct detection experiments will pin down the underlying mirror dark matter halo model parameters and its associated uncertainties along with mirror dark matter properties.

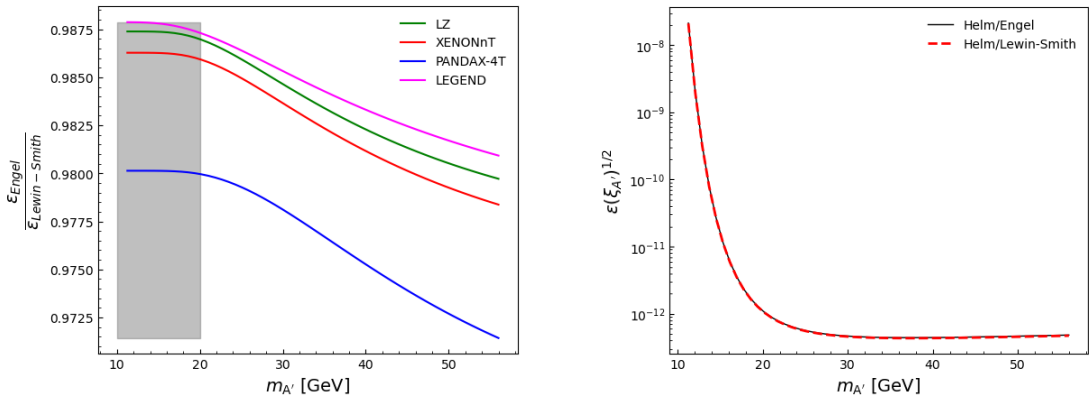


Figure 8. Left panel: Ratio of kinetic mixing sensitivity in ton size detectors for a year of exposure. ϵ_{Engel} corresponds to choice of parameters in eq.(4.7) and $\epsilon_{Lewin-Smith}$ correspond to choice of parameters in eq.(4.8) respectively. In both this cases, a halo model parameters $V_E = 235$ km/s, $v_{rot} = 220$ km/s with $\epsilon = 10^{-10}$ is taken. Right panel: 95% exclusion limit on ϵ for XENONnT using the same choices of parameters as in the left panel.

7 Conclusion

In this work, we consider halos composed of mirror atoms of various species. We modelled the velocity distribution of mirror DM particles locally a Maxwellian and we quantify mirror dark matter scattering with ordinary matter accounting for the kinetic mixing interactions. With the astrophysical and experimental considerations on kinetic mixing parameter ϵ , we estimate the available parameter space in germanium and xenon targets in the context of direct detection experiments. The effect of halo model parameters and their uncertainties are accounted for by studying the signal events and associated sensitivities have been obtained. In addition, the influence of nuclear helm form factors on signal models has been carefully examined. It is worth noting that an increase of theoretically predicted mirror events in the low energy region of the recoil spectrum can give rise to measurable nuclear and electronic recoil signals at the current threshold of detectors and corresponding kinetic mixing parameter ϵ can be measured with better accuracy. Dark matter captured by the Earth and subsequent shielding effect is not included in this work [58]. This might have a significant effect on the mirror electrons signal model, nevertheless, with the simplest model as discussed throughout the main text, a vast portion of allowed parameter space can be closely scrutinized in current direct detection experiments and forthcoming experiments as well. Our early analyses on mirror dark matter scattering with ordinary targets show appreciable promise for mirror dark sector physics and this direction suggests further exploration. Thus, we are optimistic that mirror dark matter interpretation will be tested and the whole new field of physics with mirror particle mass and interaction properties may soon unfold itself for discovery.

A Mirror nuclear form factors and kinetic mixing sensitivity

As we discussed in the main text that nuclear form factors are paramount entity that is required in computing the scattering rates. Momentum-dependent nuclear form factors $F(q^2)$ for various choices of parameterizations in nuclear radius and nuclear skin thickness are discussed in section § 4.1. With these choices of parameterization, we estimate the 95%

$\epsilon_{Lewin-Smith}$	ϵ_{Engel}
$2.125 \cdot 10^{-8}$	$2.096 \cdot 10^{-8}$
$1.970 \cdot 10^{-9}$	$1.943 \cdot 10^{-9}$
$3.209 \cdot 10^{-10}$	$3.166 \cdot 10^{-10}$
$7.938 \cdot 10^{-11}$	$7.829 \cdot 10^{-11}$
$2.686 \cdot 10^{-11}$	$2.649 \cdot 10^{-11}$
$1.154 \cdot 10^{-11}$	$1.138 \cdot 10^{-11}$
$5.948 \cdot 10^{-12}$	$5.866 \cdot 10^{-12}$
$3.530 \cdot 10^{-12}$	$3.482 \cdot 10^{-12}$
$2.337 \cdot 10^{-12}$	$2.305 \cdot 10^{-12}$
$1.684 \cdot 10^{-12}$	$1.661 \cdot 10^{-12}$
$1.298 \cdot 10^{-12}$	$1.280 \cdot 10^{-12}$
$1.053 \cdot 10^{-12}$	$1.038 \cdot 10^{-12}$

Table 4. 95% exclusion limits on kinetic mixing sensitivity in the allowed parameter space over mass scale of (11 – 20) GeV at XENONnT one year of exposure with halo model parameters: $v_E = 235$ km/s, and $v_{rot} = 220$ km/s.

exclusion limit at XENONnT using the halo model parameters under considerations: Earth’s velocity $v_E = 235$ km/s and galactic rotational velocity $v_{rot} = 220$ km/s. Similar exclusion table can be obtained for other detectors i.e. LEGEND, LZ, and PANDAX-4T.

B Lindhard model

In dark matter direct detection, often we require to calculate electronic equivalent energy (E_{ee}) and corresponding nuclear recoil (E_R) in the detector. One can convert nuclear recoil to electronic equivalent and vice versa using the Lindhard model as follows [59, 60],

$$L(E_R) = \frac{kg(\epsilon)}{1 + kg(\epsilon)} \quad (\text{B.1})$$

$$g(\epsilon) = 3\epsilon^{1.5} + 0.7\epsilon^{0.6} + \epsilon \quad (\text{B.2})$$

$$E_{ee} = L(E_R) \cdot E_R \quad (\text{B.3})$$

with $\epsilon = 11.5(E_R/\text{KeV})Z^{-7/3}$. It is clear that ϵ in eq.(C.1) has a different meaning, it is not the kinetic mixing parameter ϵ as discussed in the main text in section § 4. The quantity $g(\epsilon)$ is the function of the recoil can be computed using the Thomas-Fermi screening function. The parameter k is a proportionality constant. The optimized value of $k = 0.177 \pm 0.0060$ is reported in [61] however $k = 0.166$ is also well-accepted. Generally, it may range (0.1 – 0.2) more detail in [62].

Acknowledgments

We greatly appreciate Micheal Graesser for reading the manuscript and providing us with a insightful comments. The author would like to thank Michael Gold and Ralph Massaraczyk for fruitful discussions.

References

- [1] V.C. Rubin, W.K. Ford, Jr. and N. Thonnard, *Extended rotation curves of high-luminosity spiral galaxies. IV. Systematic dynamical properties, Sa through Sc*, *Astrophys. J. Lett.* **225** (1978) L107.
- [2] XENON collaboration, *First Dark Matter Search with Nuclear Recoils from the XENONnT Experiment*, *Phys. Rev. Lett.* **131** (2023) 041003 [2303.14729].
- [3] LUX-ZEPLIN COLLABORATION collaboration, *First dark matter search results from the lux-zeplin (lz) experiment*, *Phys. Rev. Lett.* **131** (2023) 041002.
- [4] PANDAX-4T collaboration, *Dark Matter Search Results from the PandaX-4T Commissioning Run*, *Phys. Rev. Lett.* **127** (2021) 261802 [2107.13438].
- [5] DARWIN collaboration, *DARWIN: towards the ultimate dark matter detector*, *JCAP* **11** (2016) 017 [1606.07001].
- [6] C.E. Aalseth, F. Acerbi, P. Agnes, I.F.M. Albuquerque, T. Alexander, A. Alici et al., *Darkside-20k: A 20 tonne two-phase lar tpc for direct dark matter detection at lngs*, *The European Physical Journal Plus* **133** (2018) .
- [7] PLANCK collaboration, *Planck 2018 results. VI. Cosmological parameters*, *Astron. Astrophys.* **641** (2020) A6 [1807.06209].
- [8] L. Roszkowski, E.M. Sessolo and S. Trojanowski, *WIMP dark matter candidates and searches—current status and future prospects*, *Rept. Prog. Phys.* **81** (2018) 066201 [1707.06277].
- [9] G. Bertone, D. Hooper and J. Silk, *Particle dark matter: Evidence, candidates and constraints*, *Phys. Rept.* **405** (2005) 279 [hep-ph/0404175].
- [10] L. Bergstrom, *Dark Matter Candidates*, *New J. Phys.* **11** (2009) 105006 [0903.4849].
- [11] T.D. Lee and C.-N. Yang, *Question of Parity Conservation in Weak Interactions*, *Phys. Rev.* **104** (1956) 254.
- [12] Z. Berezhiani and A. Gazizov, *Neutron Oscillations to Parallel World: Earlier End to the Cosmic Ray Spectrum?*, *Eur. Phys. J. C* **72** (2012) 2111 [1109.3725].
- [13] R. Foot and S. Vagnozzi, *Solving the small-scale structure puzzles with dissipative dark matter*, *JCAP* **07** (2016) 013 [1602.02467].
- [14] Z. Berezhiani, D. Comelli and F.L. Villante, *The Early mirror universe: Inflation, baryogenesis, nucleosynthesis and dark matter*, *Phys. Lett. B* **503** (2001) 362 [hep-ph/0008105].
- [15] I.Y. Kobzarev, L.B. Okun and I.Y. Pomeranchuk, *On the possibility of experimental observation of mirror particles*, *Sov. J. Nucl. Phys.* **3** (1966) 837.
- [16] R. Cerulli, P. Villar, F. Cappella, R. Bernabei, P. Belli, A. Incicchitti et al., *DAMA annual modulation and mirror Dark Matter*, *Eur. Phys. J. C* **77** (2017) 83 [1701.08590].
- [17] R. Foot, *Mirror dark matter: Cosmology, galaxy structure and direct detection*, *Int. J. Mod. Phys. A* **29** (2014) 1430013 [1401.3965].
- [18] R. Foot and S. Vagnozzi, *Dissipative hidden sector dark matter*, *Phys. Rev. D* **91** (2015) 023512 [1409.7174].

- [19] G.G. Raffelt, *Stars as laboratories for fundamental physics: The astrophysics of neutrinos, axions, and other weakly interacting particles*, University of Chicago press (1996).
- [20] J.D. Clarke and R. Foot, *Mirror dark matter will be confirmed or excluded by XENON1T*, *Physics Letters B* **766** (2017) 29 [[1606.09063](#)].
- [21] C. McCabe, *The Astrophysical Uncertainties Of Dark Matter Direct Detection Experiments*, *Phys. Rev. D* **82** (2010) 023530 [[1005.0579](#)].
- [22] A.J.K. Chua, D.T. Wickramasinghe and L. Ferrario, *Galactic Escape Speeds in Mirror and Cold Dark Matter Models*, *Eur. Phys. J. C* **73** (2013) 2259 [[1301.3517](#)].
- [23] J. Bramante, P.J. Fox, G.D. Kribs and A. Martin, *Inelastic frontier: Discovering dark matter at high recoil energy*, *Phys. Rev. D* **94** (2016) 115026 [[1608.02662](#)].
- [24] S.K. Lee, M. Lisanti and B.R. Safdi, *Dark-Matter Harmonics Beyond Annual Modulation*, *JCAP* **11** (2013) 033 [[1307.5323](#)].
- [25] P. Ciarcelluti and R. Foot, *Primordial He' abundance implied by the mirror dark matter interpretation of the DAMA/Libra signal*, *Phys. Lett. B* **690** (2010) 462 [[1003.0880](#)].
- [26] K. Freese, M. Lisanti and C. Savage, *Colloquium: Annual modulation of dark matter*, *Rev. Mod. Phys.* **85** (2013) 1561 [[1209.3339](#)].
- [27] D.N. Spergel, *Motion of the earth and the detection of weakly interacting massive particles*, *Phys. Rev. D* **37** (1988) 1353.
- [28] R. Foot, *DAMA annual modulation from electron recoils*, *Phys. Lett. B* **785** (2018) 403 [[1804.11018](#)].
- [29] R. Foot, *Direct detection experiments explained with mirror dark matter*, *Phys. Lett. B* **728** (2014) 45 [[1305.4316](#)].
- [30] R. Foot and S. Mitra, *Mirror matter in the solar system: New evidence for mirror matter from EROS*, *Astropart. Phys.* **19** (2003) 739 [[astro-ph/0211067](#)].
- [31] S. Orrigo, L. Alvarez-Ruso and C. Peña-Garay, *A new approach to nuclear form factors for direct dark matter searches*, *Nuclear and Particle Physics Proceedings* **273-275** (2016) 414.
- [32] R.H. Helm, *Inelastic and elastic scattering of 187-mev electrons from selected even-even nuclei*, *Phys. Rev.* **104** (1956) 1466.
- [33] J. Engel, S. Pittel and P. Vogel, *Nuclear physics of dark matter detection*, *Int. J. Mod. Phys. E* **1** (1992) 1.
- [34] J. Engel, *Nuclear form-factors for the scattering of weakly interacting massive particles*, *Phys. Lett. B* **264** (1991) 114.
- [35] J.D. Lewin and P.F. Smith, *Review of mathematics, numerical factors, and corrections for dark matter experiments based on elastic nuclear recoil*, *Astroparticle Physics* **6** (1996) 87.
- [36] PARTICLE DATA GROUP collaboration, *Review of particle physics*, *Phys. Rev. D* **98** (2018) 030001.
- [37] M. Schumann, *Direct Detection of WIMP Dark Matter: Concepts and Status*, *J. Phys. G* **46** (2019) 103003 [[1903.03026](#)].
- [38] A.H.G. Peter, V. Gluscevic, A.M. Green, B.J. Kavanagh and S.K. Lee, *WIMP physics with ensembles of direct-detection experiments*, *Phys. Dark Univ.* **5-6** (2014) 45 [[1310.7039](#)].
- [39] M.W. Goodman and E. Witten, *Detectability of Certain Dark Matter Candidates*, *Phys. Rev. D* **31** (1985) 3059.
- [40] G. Arcadi, M. Dutra, P. Ghosh, M. Lindner, Y. Mambrini, M. Pierre et al., *The waning of the WIMP? A review of models, searches, and constraints*, *Eur. Phys. J. C* **78** (2018) 203 [[1703.07364](#)].

- [41] GERDA collaboration, *First Search for Bosonic Superweakly Interacting Massive Particles with Masses up to 1 MeV/c² with GERDA*, *Phys. Rev. Lett.* **125** (2020) 011801 [[2005.14184](#)].
- [42] MAJORANA collaboration, *A Dark Matter Search with MALBEK*, *Phys. Procedia* **61** (2015) 77 [[1407.2238](#)].
- [43] SUPERCDMS collaboration, *Search for low-mass dark matter via bremsstrahlung radiation and the Migdal effect in SuperCDMS*, *Phys. Rev. D* **107** (2023) 112013 [[2302.09115](#)].
- [44] GERDA collaboration, *The GERDA experiment for the search of $0\nu\beta\beta$ decay in ⁷⁶Ge*, *Eur. Phys. J. C* **73** (2013) 2330 [[1212.4067](#)].
- [45] LEGEND collaboration, *LEGEND: The future of neutrinoless double-beta decay search with germanium detectors*, *J. Phys. Conf. Ser.* **1468** (2020) 012111.
- [46] MAJORANA COLLABORATION collaboration, *Exotic dark matter search with the majorana demonstrator*, *Phys. Rev. Lett.* **132** (2024) 041001.
- [47] J. Aalbers et al., *A next-generation liquid xenon observatory for dark matter and neutrino physics*, *J. Phys. G* **50** (2023) 013001 [[2203.02309](#)].
- [48] PANDAX collaboration, *Search for Light Dark Matter from the Atmosphere in PandaX-4T*, *Phys. Rev. Lett.* **131** (2023) 041001 [[2301.03010](#)].
- [49] XENON collaboration, *Projected WIMP sensitivity of the XENONnT dark matter experiment*, *JCAP* **11** (2020) 031 [[2007.08796](#)].
- [50] NEXT collaboration, *Demonstration of neutrinoless double beta decay searches in gaseous xenon with NEXT*, *JHEP* **09** (2023) 190 [[2305.09435](#)].
- [51] X. Chen et al., *PandaX-III: Searching for neutrinoless double beta decay with high pressure¹³⁶Xe gas time projection chambers*, *Sci. China Phys. Mech. Astron.* **60** (2017) 061011 [[1610.08883](#)].
- [52] D. Ramírez García, *Simulating the XENONnT dark matter experiment: backgrounds and WIMP sensitivity*, Ph.D. thesis, Freiburg U., 2022. [10.6094/UNIFR/228338](#).
- [53] LZ collaboration, *Background determination for the LUX-ZEPLIN dark matter experiment*, *Phys. Rev. D* **108** (2023) 012010 [[2211.17120](#)].
- [54] PANDAX collaboration, *Dark matter direct search sensitivity of the PandaX-4T experiment*, *Sci. China Phys. Mech. Astron.* **62** (2019) 31011 [[1806.02229](#)].
- [55] XENON collaboration, *Excess electronic recoil events in XENON1T*, *Phys. Rev. D* **102** (2020) 072004 [[2006.09721](#)].
- [56] C. Vigo, L. Gerchow, L. Liskay, A. Rubbia and P. Crivelli, *First search for invisible decays of orthopositronium confined in a vacuum cavity*, *Phys. Rev. D* **97** (2018) 092008 [[1803.05744](#)].
- [57] LUX collaboration, *First direct detection constraint on mirror dark matter kinetic mixing using LUX 2013 data*, *Phys. Rev. D* **101** (2020) 012003 [[1908.03479](#)].
- [58] R. Foot, *Shielding of a direct detection experiment and implications for the DAMA annual modulation signal*, *Phys. Lett. B* **789** (2019) 592 [[1806.04293](#)].
- [59] J. Lindhard, V. Nielsen, M. Scharff and P.V. Thomsen, *Integral equations governing radiation effects. (notes on atomic collisions, iii)*, *Kgl. Danske Videnskab., Selskab. Mat. Fys. Medd.*, Vol: 33: No. 10 (1963) .
- [60] LUX collaboration, *Low-energy (0.7-74 keV) nuclear recoil calibration of the LUX dark matter experiment using D-D neutron scattering kinematics*, [1608.05381](#).
- [61] LUX collaboration, *Low-energy (0.7-74 keV) nuclear recoil calibration of the LUX dark matter experiment using D-D neutron scattering kinematics*, [1608.05381](#).

- [62] P. Sorensen and C.E. Dahl, *Nuclear recoil energy scale in liquid xenon with application to the direct detection of dark matter*, *Phys. Rev. D* **83** (2011) 063501 [[1101.6080](#)].